Geometric Neural Diffusion Processes

Vincent Dutordoir

15th September 2023

Alan Turing Institute
Uncertainty Quantification for Generative Modelling

UNIVERSITY OF CAMBRIDGE

Papers of Reference and Collaborators

Neural Diffusion Processes. ICML 2023.


Vincent Dutordoir


Alan Saul


Zoubin Ghahramani


Fergus Simpson

Geometric Neural Diffusion Processes. Under submission.


Émile Mathieu*


Vincent Dutordoir*


Michael Hutchinson*


Valentin De Bortoli


Yee Whye Teh


Richard E. Turner

Rise of Diffusion Models

Figure 1: Samples from stable diffusion

Goal

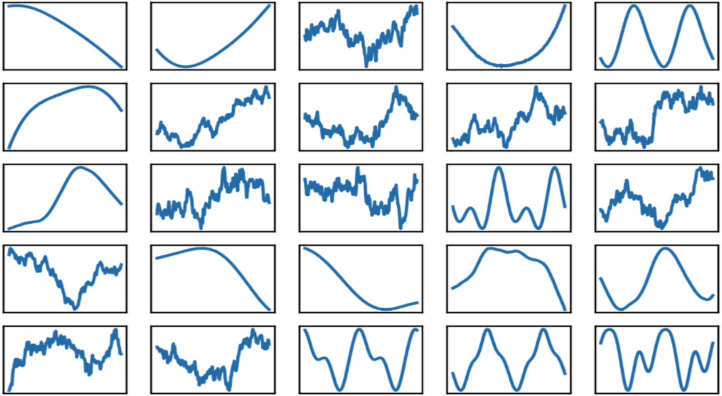

Goal

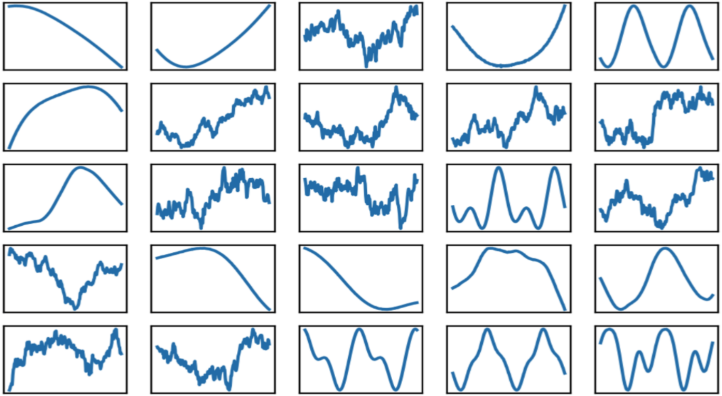

Why

- Many physical and natural phenomena are better characterised as functions.
- Meta-learn and treat limited data as originating from a function.

Feature Fields: $f : \mathcal{X} \to \mathbb{R}^d$

- Mathematical framework for modelling natural phenomena.
- Examples: Temperature $f : \mathcal{X} \to \mathbb{R}$, and wind direction on globe $f : \mathcal{S}^2 \to T\mathcal{S}^2$.

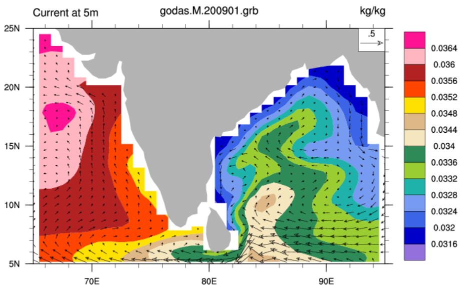

(a) Temperature map and wind vector fields.

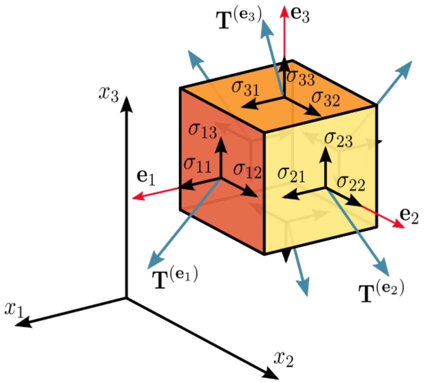

(b) 3D stress tensor (type-2) diagram.

Prior invariances

Encode invariances w.r.t. group transformations. For a group G, we want $\forall g \in G$

$$p(f) = p(g \cdot f) \quad \text{with} \quad g \cdot f = \rho(g) f(g^{-1} x).$$

Prior invariances

Encode invariances w.r.t. group transformations. For a group G, we want $\forall g \in G$

$$p(f) = p(g \cdot f) \quad \text{with} \quad g \cdot f = \rho(g) f(g^{-1}x).$$

Examples translation invariance (stationarity) and rotational invariance.

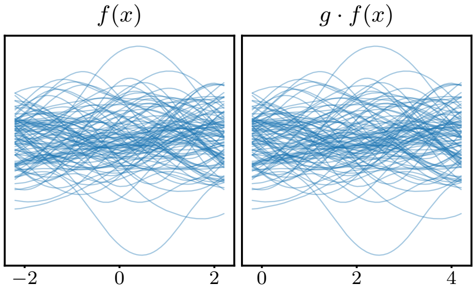

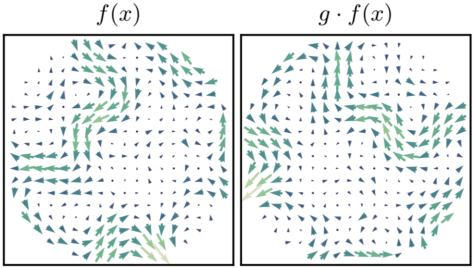

Conditional process

- Interested in the conditional process given a set of observations $\mathcal{C} = \{(x_n, y_n)\}_{n=1}$.
- If the prior is G-invariant, then the conditional is G-equivariant:

$$p(f \mid \mathcal{C}) = p(g \cdot f | g \cdot \mathcal{C}) \quad \text{where} \quad g \cdot \mathcal{C} = \{(g \cdot x_n, \rho(g) y_n)\}.$$

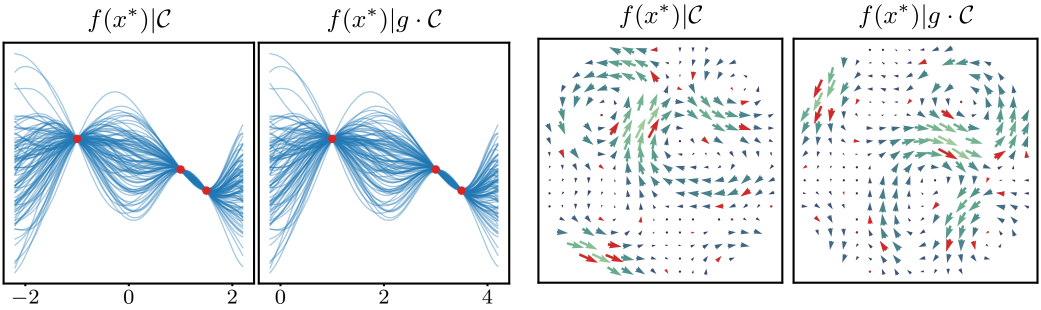

Continuous diffusion models

Principles of continuous diffusion models

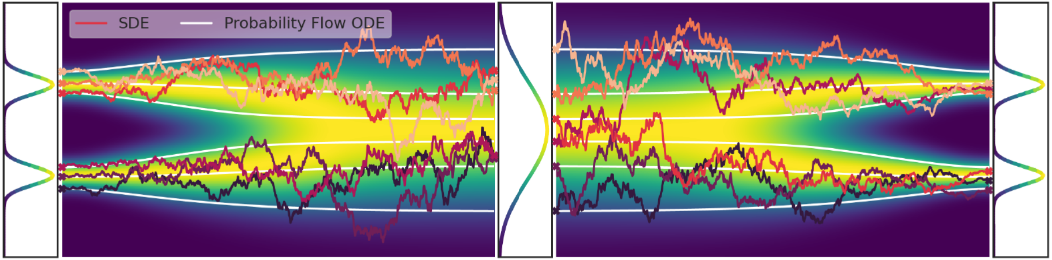

Figure 5: (Song et al., 2021)

- Idea: Destruct data with *continuous* series of noise.
- Do this by constructing an **SDE** forward noising process $(\mathbf{Y}_t)_{t \in [0,T]}$.
- Have this noising converge to a **known distribution**.
- **Invert** this SDE noising process to get **denoising** process.

Continuous noising processes

The **Forward process** progressively perturbs the data following a SDE

$$\mathrm{d}\mathbf{Y}_t = \boxed{-\mathbf{Y}_t}\,\mathrm{d}t + \boxed{\sqrt{2}}\,\mathrm{d}\mathbf{B}_t, \tag{1}$$

where $\mathbf{B}_t$ is Brownian motion (think of it conceptually as $\mathrm{d}\mathbf{B}_t/\mathrm{d}t \sim \mathcal{N}(0, \mathrm{d}t)$).

Example: 2D Gaussian data

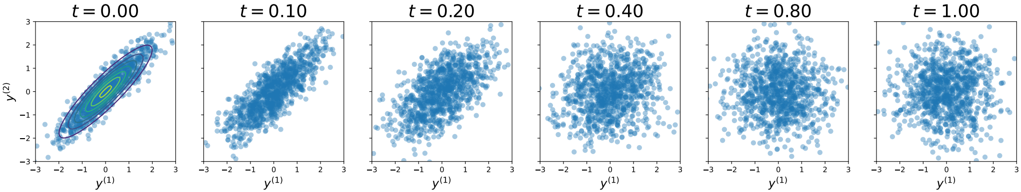

Figure 6: Forward process

Continuous score-based models: Time reversal process

Theorem 1: (Cattiaux et al., 2021; Haussmann and Pardoux, 1986)

The time-reversed process $(\bar{\mathbf{Y}}_t)_{t\geq 0} = (\mathbf{Y}_{T-t})_{t\in[0,T]}$, with forward process $\mathrm{d}\mathbf{Y}_t = -\mathbf{Y}_t \mathrm{d}t + \sqrt{2}\mathrm{d}\mathbf{B}_t$, also satisfies an SDE given by

$$\mathrm{d}\bar{\mathbf{Y}}_t = \left[-\bar{\mathbf{Y}}_t + 2\,\nabla \log p_{T-t}(\bar{\mathbf{Y}}_t)\right]\mathrm{d}t + \sqrt{2}\mathrm{d}\mathbf{B}_t,$$

assuming $\bar{\mathbf{Y}}_0$ is distributed the same as $\mathbf{Y}_T$.

Continuous score-based models: Time reversal process

Theorem 2: (Cattiaux et al., 2021; Haussmann and Pardoux, 1986)

The time-reversed process $(\bar{\mathbf{Y}}_t)_{t\geq 0} = (\mathbf{Y}_{T-t})_{t\in[0,T]}$, with forward process $\mathrm{d}\mathbf{Y}_t = -\mathbf{Y}_t \mathrm{d}t + \sqrt{2}\mathrm{d}\mathbf{B}_t$, also satisfies an SDE given by

$$\mathrm{d}\bar{\mathbf{Y}}_t = \left[-\bar{\mathbf{Y}}_t + 2\,\nabla \log p_{T-t}(\bar{\mathbf{Y}}_t)\right] \mathrm{d}t + \sqrt{2}\mathrm{d}\mathbf{B}_t,$$

assuming $\bar{\mathbf{Y}}_0$ is distributed the same as $\mathbf{Y}_T$.

Problem The Stein score $\nabla \log p_t = \nabla \log \int p_{data}(\mathbf{Y}_0) p_{t|0}(\mathbf{Y}_t \mid \mathbf{Y}_0) \mathrm{d}\mathbf{Y}_0$ is intractable.

Denoising Score Matching

Parameterise score using neural network $\mathbf{s}_\theta : [0, T] \times \mathbb{R}^d \to \mathbb{R}^d$ and learn score using the Denoising Score Matching objective

$$\mathcal{L}(\theta) = \mathbb{E}[\| \mathrm{s}_\theta(t, \mathbf{Y}_t) - \nabla \log p_t(\mathbf{Y}_t | \mathbf{Y}_0)\|^2]. \tag{2}$$

Example

$$\mathrm{d}\bar{\mathbf{Y}}_t = \left[-\bar{\mathbf{Y}}_t + 2\, s_\theta(t, \bar{\mathbf{Y}}_t)\right] \mathrm{d}t + \sqrt{2}\mathrm{d}\mathbf{B}_t,$$

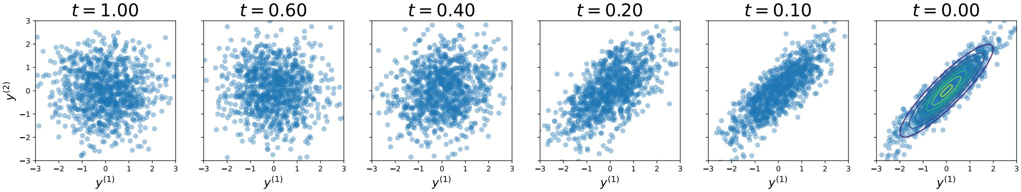

Figure 7: Reverse process

Diffusion on Function Spaces

Continuous noising process

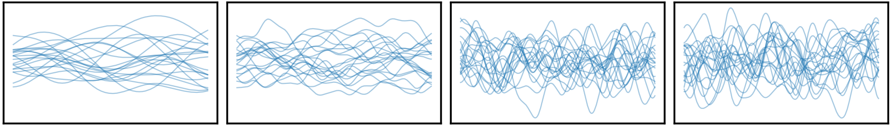

We construct the forward **noising process** $(\mathbf{Y}_t(x))_{t\geq 0} \triangleq (\mathbf{Y}_t(x^1), \dots, \mathbf{Y}_t(x^n))_{t\geq 0}$ defined by the multivariate SDE (multivariate Ornstein-Uhlenbeck process)

$$\mathrm{d}\mathbf{Y}_t(x) = \frac{1}{2}\left\{m(x) - \mathbf{Y}_t(x)\right\}\beta_t \,\mathrm{d}t + \beta_t^{1/2}\mathrm{K}(x,x)^{1/2}\,\mathrm{d}\mathbf{B}_t, \tag{3}$$

where $\mathrm{K}(x,x)_{i,j} = k(x^i, x^j)$ with $k : \mathcal{X} \times \mathcal{X} \to \mathbb{R}$ a kernel and $m : \mathcal{X} \to \mathcal{Y}$.

Continuous noising process

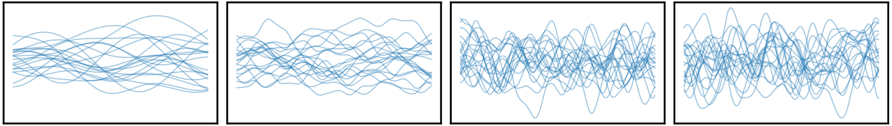

We construct the forward **noising process** $(\mathbf{Y}_t(x))_{t\geq 0} \triangleq (\mathbf{Y}_t(x^1), \ldots, \mathbf{Y}_t(x^n))_{t\geq 0}$ defined by the multivariate SDE (multivariate Ornstein-Uhlenbeck process)

$$\mathrm{d}\mathbf{Y}_t(x) = \frac{1}{2}\{m(x) - \mathbf{Y}_t(x)\}\,\beta_t\,\mathrm{d}t + \beta_t^{1/2}\mathrm{K}(x,x)^{1/2}\,\mathrm{d}\mathbf{B}_t, \tag{3}$$

where $\mathrm{K}(x,x)_{i,j} = k(x^i, x^j)$ with $k : \mathcal{X} \times \mathcal{X} \to \mathbb{R}$ a kernel and $m : \mathcal{X} \to \mathcal{Y}$.

- $\mathbf{Y}_t(x) \to \mathrm{N}(m(x), \mathrm{K}(x,x))$ with geometric rate, for any $x \in \mathcal{X}^n$.
- $\mathbf{Y}_t \to \mathrm{GP}(m,k) \triangleq \mathbf{Y}_\infty$ (Phillips et al., 2022).

Continuous noising process

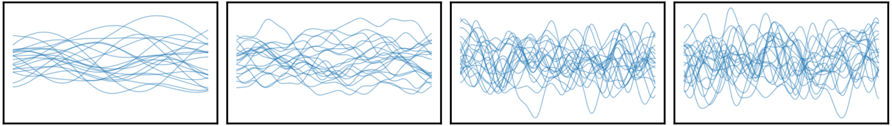

We construct the forward **noising process** $(\mathbf{Y}_t(x))_{t \geq 0} \triangleq (\mathbf{Y}_t(x^1), \ldots, \mathbf{Y}_t(x^n))_{t \geq 0}$ defined by the multivariate SDE (multivariate Ornstein-Uhlenbeck process)

$$\mathrm{d}\mathbf{Y}_t(x) = \frac{1}{2}\left\{m(x) - \mathbf{Y}_t(x)\right\}\beta_t \,\mathrm{d}t + \beta_t^{1/2}\mathrm{K}(x,x)^{1/2}\,\mathrm{d}\mathbf{B}_t, \tag{3}$$

where $\mathrm{K}(x,x)_{i,j} = k(x^i, x^j)$ with $k : \mathcal{X} \times \mathcal{X} \to \mathbb{R}$ a kernel and $m : \mathcal{X} \to \mathcal{Y}$.

- $\mathbf{Y}_t(x) \to \mathrm{N}(m(x), \mathrm{K}(x,x))$ with geometric rate, for any $x \in \mathcal{X}^n$.
- $\mathbf{Y}_t \to \mathrm{GP}(m,k) \triangleq \mathbf{Y}_\infty$ (Phillips et al., 2022).
- $\mathbf{Y}_t$ interpolates between $\mathbf{Y}_0$ and $\mathbf{Y}_\infty$.
- $\mathbf{Y}_t(x)|\boldsymbol{y}_0 = \mathrm{N}(m_t(x;\boldsymbol{y}_0), \mathrm{K}_t(x,x;\boldsymbol{y}_0))$ for any $x \in \mathcal{X}^n$.

Continuous noising process

$$k(x, x') = k_{\mathrm{rbf}}(x, x') = \sigma^2 \exp\left(\frac{\|x - x'\|^2}{2l^2}\right), \text{ with } l = 1.$$

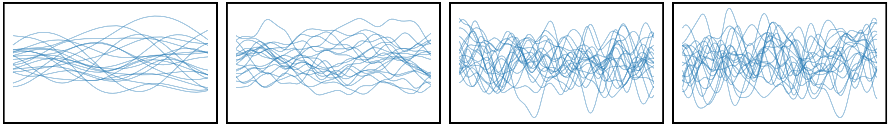

Continuous noising process

$$k(x, x') = k_{\mathrm{rbf}}(x, x') = \sigma^2 \exp\left(\frac{\|x-x'\|^2}{2l^2}\right), \text{ with } l = 1.$$

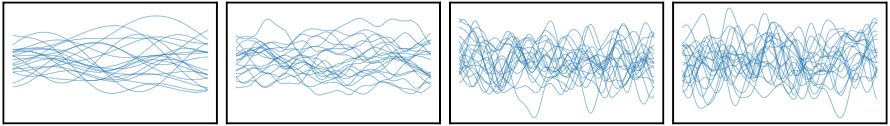

$$k(x, x') = k_{\mathrm{rbf}}(x, x'), \text{ with } l = 0.2.$$

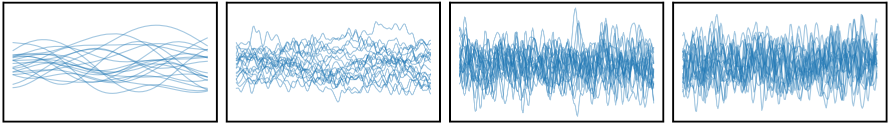

Continuous noising process

$k(x, x') = k_{\mathrm{rbf}}(x, x') = \sigma^2 \exp\left(\frac{\|x-x'\|^2}{2l^2}\right)$, with $l = 1$.

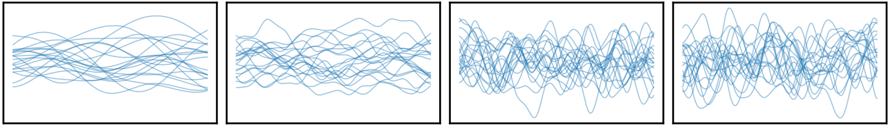

$k(x, x') = k_{\mathrm{rbf}}(x, x')$, with $l = 0.2$.

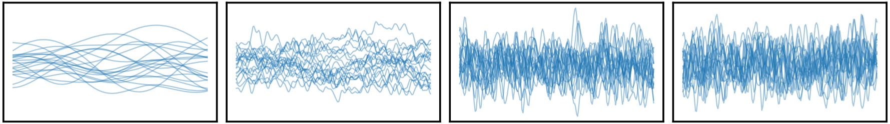

$k(x, x') = \delta_x(x')$ (The tranditional DDPM settings).

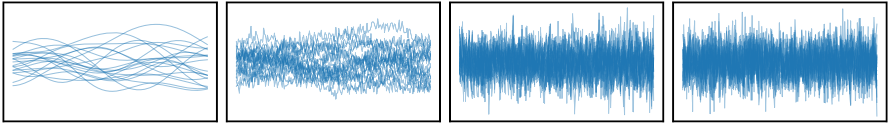

Encoding Invariances

Prior and Conditional Symmetries

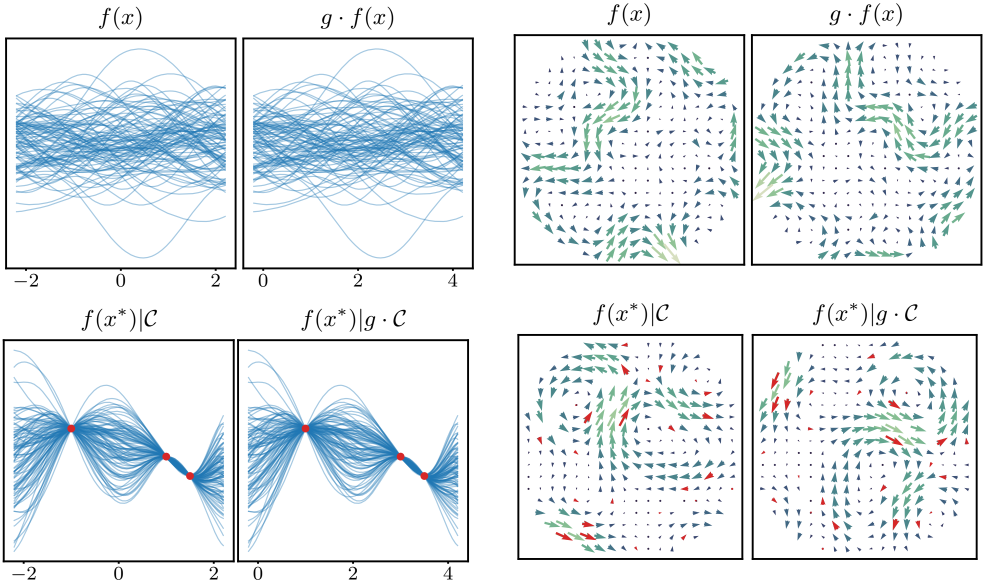

Invariant neural diffusion processes

Proposition 1: Invariant Neural Diffusion Processes

The denoising process on functions as defined above and with initial sample given by $p(\bar{\mathbf{Y}}_0) = \mathrm{GP}(m, k)$ is G-invariant if

1. m and k are both G-equivariant (i.e. G-invariant Gaussian process), i.e.

$$m(g \cdot x) = \rho(g) m(x) \quad \text{and} \quad k(g \cdot x, g \cdot x') = \rho(g) k(x, x') \rho(g)^\top,$$

2. the score network is G-equivariant vector field, i.e.

$$\mathbf{s}_\theta(t, g \cdot x, \rho(g) y) = \rho(g) \mathbf{s}_\theta(t, x, y),$$

for all $x \in \mathcal{X}, g \in G$.

Conditional Process

Conditional sampling in diffusion models

Goal: Sample from $y \sim p(\cdot \mid \mathcal{C})$ given a condition $\mathcal{C}$.

Conditional sampling in diffusion models

Goal: Sample from $y \sim p(\cdot \mid \mathcal{C})$ given a condition $\mathcal{C}$.

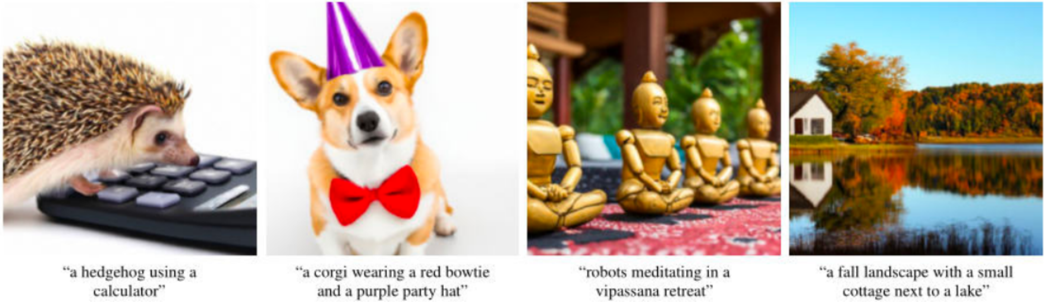

Figure 10: $p(image \mid text)$

Often the condition is a property (e.g., caption).

Conditional sampling in diffusion models for functions

Condition is a subspace of the state space: $y = (y^{(1)}, \ldots, y^{(m)})$ and $\mathcal{C} = (y^{(m+1)}, \ldots, y^{(n)})$.

Conditional sampling in diffusion models for functions

Condition is a subspace of the state space: $y = (y^{(1)}, \ldots, y^{(m)})$ and $\mathcal{C} = (y^{(m+1)}, \ldots, y^{(n)})$.

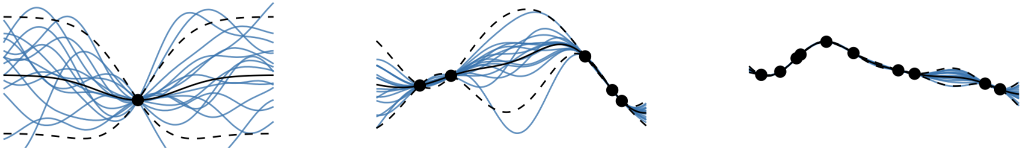

Figure 11: Conditional samples $p(y^* \mid \mathcal{C})$.

Conditional sampling in diffusion models

In the reverse process we need to follow the **Conditional Score**

$$\nabla \log p_t(\mathbf{Y}_t) \implies \nabla \log p_t(\mathbf{Y}_t \mid \mathcal{C})$$

Conditional sampling in diffusion models

In the reverse process we need to follow the **Conditional Score**

$$\nabla \log p_t(\mathbf{Y}_t) \implies \nabla \log p_t(\mathbf{Y}_t \mid \mathcal{C})$$

1. Amortisation / Classifier-free (Ramesh et al., 2022)
2. Classifier-guidance (Dhariwal and Nichol, 2021)
3. Replacement methods RePaint (Lugmayr et al., 2022)
4. Reconstruction guidance (Finzi et al., 2023)
5. SMC-based (Trippe et al., 2022)

Langevin Dynamics based Conditional Sampling

Focussing on the function setting, the context $\mathcal{C} = \mathbf{Y}_0^{\mathcal{C}}$

$$\begin{aligned}\nabla_{\mathbf{Y}_t} \log p_t(\mathbf{Y}_t \mid \mathbf{Y}_0^{\mathcal{C}}) &= \nabla_{\mathbf{Y}_t} \log p_t(\mathbf{Y}_t, \mathbf{Y}_0^{\mathcal{C}}) - \nabla_{\mathbf{Y}_t} \log p_t(\mathbf{Y}_0^{\mathcal{C}}) \\ &= \nabla_{\mathbf{Y}_t} \log p_t(\mathbf{Y}_t, \mathbf{Y}_0^{\mathcal{C}})\end{aligned}$$

Langevin Dynamics based Conditional Sampling

Focussing on the function setting, the context $\mathcal{C} = \mathbf{Y}_0^{\mathcal{C}}$

$$\begin{aligned} \nabla_{\mathbf{Y}_t} \log p_t(\mathbf{Y}_t \mid \mathbf{Y}_0^{\mathcal{C}}) &= \nabla_{\mathbf{Y}_t} \log p_t(\mathbf{Y}_t, \mathbf{Y}_0^{\mathcal{C}}) - \nabla_{\mathbf{Y}_t} \log p_t(\mathbf{Y}_0^{\mathcal{C}}) \\ &= \nabla_{\mathbf{Y}_t} \log p_t(\mathbf{Y}_t, \mathbf{Y}_0^{\mathcal{C}}) \end{aligned}$$

Predictor Use standard EM reverse process with score $s_\theta^K(t, x, [\mathbf{Y}_t, \mathbf{Y}_0^{\mathcal{C}}])$.

Corrector Correct discretisation errors using Langevin dynamics

Langevin Dynamics based Conditional Sampling

Focussing on the function setting, the context $\mathcal{C} = \mathbf{Y}_0^{\mathcal{C}}$

$$\begin{aligned}\nabla_{\mathbf{Y}_t} \log p_t(\mathbf{Y}_t \mid \mathbf{Y}_0^{\mathcal{C}}) &= \nabla_{\mathbf{Y}_t} \log p_t(\mathbf{Y}_t, \mathbf{Y}_0^{\mathcal{C}}) - \nabla_{\mathbf{Y}_t} \log p_t(\mathbf{Y}_0^{\mathcal{C}}) \\ &= \nabla_{\mathbf{Y}_t} \log p_t(\mathbf{Y}_t, \mathbf{Y}_0^{\mathcal{C}})\end{aligned}$$

Predictor Use standard EM reverse process with score $s_\theta^K(t, x, [\mathbf{Y}_t, \mathbf{Y}_0^{\mathcal{C}}])$.

Corrector Correct discretisation errors using Langevin dynamics

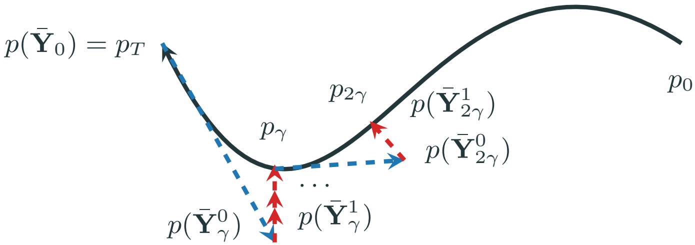

Experimental results

1D regression: Datasets

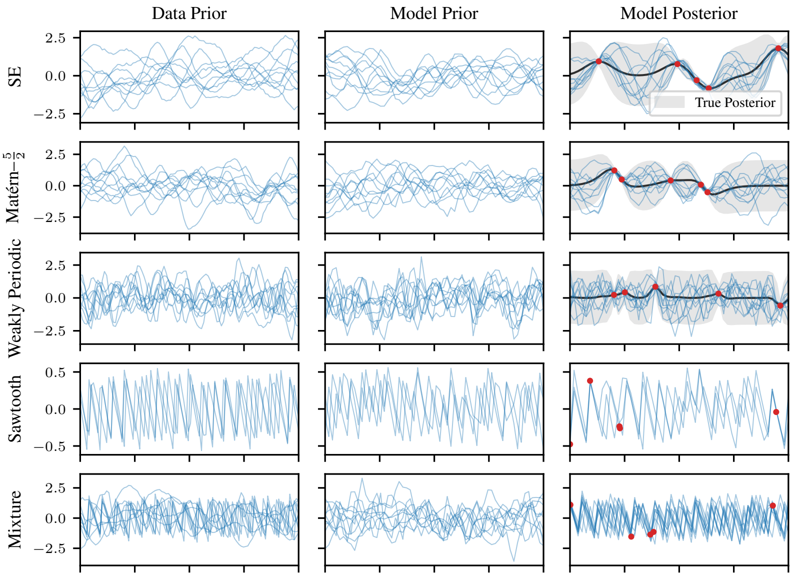

1D regression: Predictive log-likelihood (Cont'd)

Table 1: Mean test log-likelihood (TLL) (↑) $\pm$ 1 standard error estimated over 4096 test samples are reported. NP baselines from (Bruinsma et al., 2020).

		SE	Matérn($\frac{5}{2}$)	Weakly Per.	Sawtooth	Mixture
Interpolat.	GP (optimum)	$0.70{\pm}0.00$	$0.31{\pm}0.00$	$-0.32{\pm}0.00$	-	-
	T(1)−GeomNDP	$\mathbf{0.72}{\pm}0.03$	$\mathbf{0.32}{\pm}0.03$	$\mathbf{-0.38}{\pm}0.03$	$\mathbf{3.39}{\pm}0.04$	$\mathbf{0.64}{\pm}0.08$
	NDP*	$\mathbf{0.71}{\pm}0.03$	$\mathbf{0.30}{\pm}0.03$	$\mathbf{-0.37}{\pm}0.03$	$\mathbf{3.39}{\pm}0.04$	$\mathbf{0.64}{\pm}0.08$
	GNP	$\mathbf{0.70}{\pm}0.01$	$\mathbf{0.30}{\pm}0.01$	$-0.47{\pm}0.01$	$0.42{\pm}0.01$	$0.10{\pm}0.02$
	ConvNP	$-0.46{\pm}0.01$	$-0.67{\pm}0.01$	$-1.02{\pm}0.01$	$1.20{\pm}0.01$	$-0.50{\pm}0.02$
Generalisat.	GP (optimum)	$0.70{\pm}0.00$	$0.31{\pm}0.00$	$-0.32{\pm}0.00$	-	-
	T(1)−GeomNDP	$\mathbf{0.70}{\pm}0.02$	$\mathbf{0.31}{\pm}0.02$	$\mathbf{-0.38}{\pm}0.03$	$\mathbf{3.39}{\pm}0.03$	$\mathbf{0.62}{\pm}0.02$
	NDP*	*	*	*	*	*
	GNP	$\mathbf{0.69}{\pm}0.01$	$\mathbf{0.30}{\pm}0.01$	$-0.47{\pm}0.01$	$0.42{\pm}0.01$	$0.10{\pm}0.02$
	ConvNP	$-0.46{\pm}0.01$	$-0.67{\pm}0.01$	$-1.02{\pm}0.01$	$1.19{\pm}0.01$	$-0.53{\pm}0.02$

2D invariant Gaussian vector fields

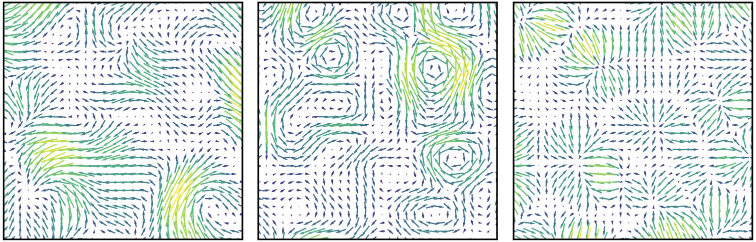

Model	SE	Curl-free	Div-free
GP	$0.56_{\pm 0.00}$	$0.66_{\pm 0.00}$	$0.66_{\pm 0.00}$
NDP*	$0.55_{\pm 0.00}$	$0.62_{\pm 0.01}$	$0.62_{\pm 0.01}$
E(2)-GeomNDP	$\mathbf{0.56_{\pm 0.01}}$	$\mathbf{0.65_{\pm 0.01}}$	$\mathbf{0.66_{\pm 0.01}}$
GP (diag.)	$-1.56_{\pm 0.00}$	$-1.47_{\pm 0.00}$	$-1.47_{\pm 0.00}$
T(2)-ConvCNP	$-1.71_{\pm 0.01}$	$-1.77_{\pm 0.01}$	$-1.76_{\pm 0.00}$
E(2)-SteerCNP	$-1.61_{\pm 0.00}$	$-1.57_{\pm 0.00}$	$-1.57_{\pm 0.01}$

2D invariant Gaussian vector fields (Cont'd)

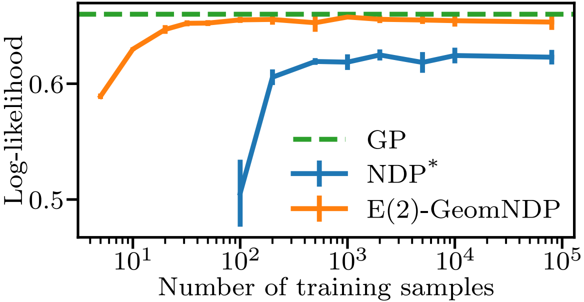

Global tropical cyclone trajectory prediction

- $f : \mathbb{R} \to \mathcal{S}^2$ with hurricane trajectory data from (Knapp et al., 2018).
- $\mathbf{Y}_t(x) = (\mathbf{Y}_t(x_1), \cdots, \mathbf{Y}_t(x_n)) \in \mathcal{M}^n$ for any $(x_1, \ldots, x_n) \in \mathbb{R}^n$
- $\mathrm{d}\mathbf{Y}_t(x_k) = -\cancelto{0}{b(\mathbf{Y}_t(x_k))}\,\mathrm{d}t + \sqrt{\beta_t}\,\mathrm{d}\mathbf{B}_t^{\mathcal{M}}\ \forall k = 1, \ldots, n$ (Bortoli et al., 2022)
- $p(\mathbf{Y}_t(x)) \underset{t\to\infty}{\longrightarrow} \mathrm{U}(\mathcal{S}^2)^{\otimes n}$.

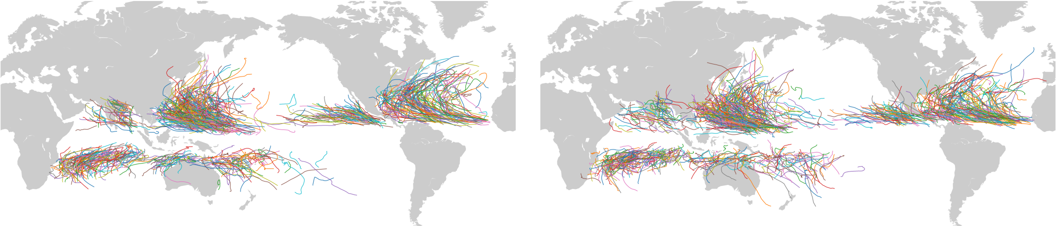

Figure 12: *Left:* 1000 samples from the training data. *Right:* 1000 samples from trained model.

Global tropical cyclone trajectory prediction (Cont'd)

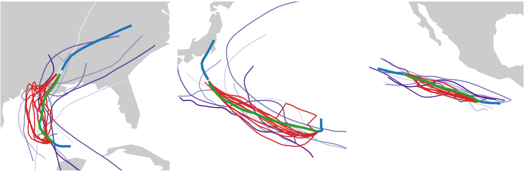

(a) Interpolation

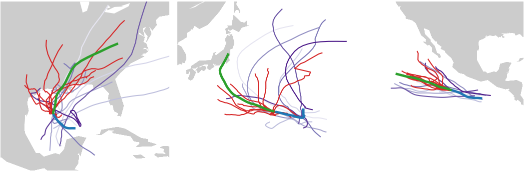

(b) Extrapolation

Model	Test data	Interpolation		Extrapolation	
	Likelihood	Likelihood	MSE (km)	Likelihood	MSE (km)
GeomNDP$(\mathbb{R} \to \mathcal{S}^2)$	$\mathbf{802}_{\pm 5}$	$\mathbf{535}_{\pm 4}$	$\mathbf{162}_{\pm 6}$	$\mathbf{536}_{\pm 4}$	$\mathbf{496}_{\pm 14}$
Stereo GP $(\mathbb{R} \to \mathbb{R}^2/\{0\})$	$393_{\pm 3}$	$266_{\pm 3}$	$2619_{\pm 13}$	$245_{\pm 2}$	$6587_{\pm 55}$
NDP $(\mathbb{R} \to \mathbb{R}^2)$	-	-	$166_{\pm 22}$	-	$769_{\pm 48}$
GP $(\mathbb{R} \to \mathbb{R}^2)$	-	-	$6852_{\pm 41}$	-	$8138_{\pm 87}$

Recap: Geometric diffusion neural processes

- Aim: probabilistic model over features fields.
- Constructed diffusion models over function space by correlating finite marginals
- Incorporating group invariance by
  - targetting invariant Gaussian processes and
  - parameterising the score with an equivariant neural network
- Sampling from the conditional process with Langevin corrector
- Empirically demonstrated modelling capacity on scalar and vector fields, with Euclidean and spherical output space

Thank you for your attention. Questions?

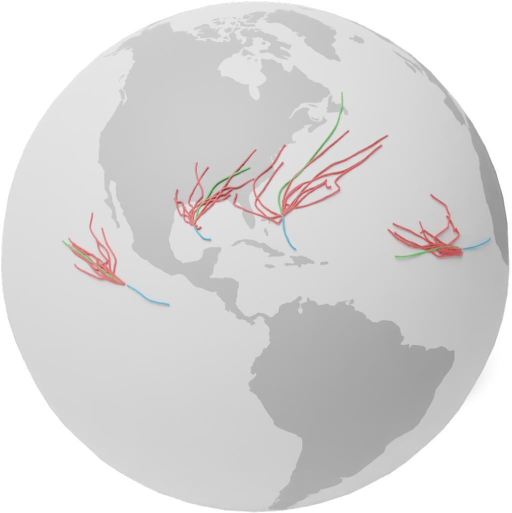

Credits to Michael Hutchinson for this 3D render.

References

V. D. Bortoli, E. Mathieu, M. J. Hutchinson, J. Thornton, Y. W. Teh, and A. Doucet. Riemannian Score-Based Generative Modelling. In *Thirty-Sixth Conference on Neural Information Processing Systems*, 2022. Cited on page 41.

W. Bruinsma, J. Requeima, A. Y. K. Foong, J. Gordon, and R. E. Turner. Gaussian Neural Processes. In *3rd Symposium on Advances in Approximate Bayesian Inference*, Feb. 2020. Cited on page 38.

P. Cattiaux, G. Conforti, I. Gentil, and C. Léonard. Time reversal of diffusion processes under a finite entropy condition. *arXiv preprint arXiv:2104.07708*, 2021. Cited on pages 13, 14.

P. Dhariwal and A. Nichol. Diffusion Models Beat GANs on Image Synthesis. 2021. arXiv: `2105.05233 [cs.LG]`. Cited on pages 31, 32.

M. A. Finzi, A. Boral, A. G. Wilson, F. Sha, and L. Zepeda-Núñez. User-defined Event Sampling and Uncertainty Quantification in Diffusion Models for Physical Dynamical Systems. In *International Conference on Machine Learning*, pages 10136–10152. PMLR, 2023. Cited on pages 31, 32.

U. G. Haussmann and E. Pardoux. Time reversal of diffusions. *The Annals of Probability*, 14(4):1188–1205, 1986. Cited on pages 13, 14.

H. J. Knapp Kenneth R. Diamond, J. P. Kossin, M. C. Kruk, and C. J. I. Schreck. International Best Track Archive for Climate Stewardship (IBTrACS) Project, Version 4. Technical report, NOAA National Centers for Environmental Information, 2018. DOI: `https://doi.org/10.25921/82ty-9e16`. Cited on page 41.

A. Lugmayr, M. Danelljan, A. Romero, F. Yu, R. Timofte, and L. Van Gool. Repaint: Inpainting using denoising diffusion probabilistic models. In *Proceedings of the*

IEEE/CVF Conference on Computer Vision and Pattern Recognition, pages 11461–11471, 2022. Cited on pages 31, 32.

A. Phillips, T. Seror, M. Hutchinson, V. De Bortoli, A. Doucet, and E. Mathieu. Spectral Diffusion Processes. Nov. 2022. URL: `http://arxiv.org/abs/2209.14125`. Cited on pages 17–19.

A. Ramesh, P. Dhariwal, A. Nichol, C. Chu, and M. Chen. Hierarchical Text-Conditional Image Generation with CLIP Latents. Apr. 2022. DOI: `10.48550/arXiv.2204.06125`. Cited on pages 31, 32.

Y. Song, J. Sohl-Dickstein, D. P. Kingma, A. Kumar, S. Ermon, and B. Poole. Score-Based Generative Modeling through Stochastic Differential Equations. In *International Conference on Learning Representations*, 2021. Cited on page 11.

B. L. Trippe, J. Yim, D. Tischer, T. Broderick, D. Baker, R. Barzilay, and T. Jaakkola. Diffusion Probabilistic Modeling of Protein Backbones in 3D for the Motif-Scaffolding Problem. June 2022. DOI: 10.48550/arXiv.2206.04119. Cited on pages 31, 32.